

## The Crystal Structure of Amesite\*

BY HUGO STEINFINK AND GEORGE BRUNTON

Shell Development Company, Houston, Texas, U.S.A.

(Received 1 August 1955 and in revised form 10 October 1955)

The crystal structure of the hydrous magnesium aluminum silicate, amesite, has been determined. X-ray precession and Weissenberg photographs of single crystals have been obtained. The crystal system is hexagonal, the space group is  $P6_3$ , and the unit cell dimensions are  $a = 5.31 \pm 0.01$ ,  $c = 14.04 \pm 0.02$  Å. There are two 'molecules' of the formula  $(Mg_2Al)(SiAl)O_5(OH)_4$  in the unit cell.

The  $(0k\bar{l})$  and  $(hki0)$  electron-density projections were evaluated and from them the parameters of the atoms were obtained. The arrangement of the atomic planes follows a kaolinite type of stacking. The kaolin-type layers are held together in the crystal by hydrogen bonds 2.97 Å long.

The reported development of an olivine phase from amesite at 700° C. is shown to be incorrect. The appearance of a strong 'olivine' line in the powder diffraction diagram is shown to be a diffuse reflection caused by disorder in the crystal at the elevated temperature.

### Introduction

Amesite has aroused considerable interest and has been extensively investigated, in spite of its relative rareness. McMurchy (1934), in his investigation of the chlorite minerals, noted that the powder pattern of amesite differed from the patterns of other chlorites, and that its structure could not be similar to a chlorite arrangement. Many investigators maintained that, because of the large amount of magnesium present in amesite, its structure must resemble that of chlorite. Pauling (1930) had pointed out that in the magnesium analogue of kaolinite the different values of the fundamental translations of the brucite layer ( $a = 5.40$  Å in brucite) and of the layer formed by the silicon tetrahedra ( $a = 5.03$  Å as in  $\beta$ -cristobalite) would cause a curvature of the kaolinite unit if the two layers were superimposed. The strain between the two layers is greatly reduced when the dimensions of the tetrahedral layer expand owing to the replacement of silicon by aluminum and the octahedral layer contracts because of the replacement of magnesium by aluminum. Gruner (1944) investigated amesite and from the intensities of the basal reflections concluded that amesite was essentially a kaolin-type mineral, but postulated an interstratification of chlorite-type layers to the extent of about 1 chlorite to every 10–16 kaolin layers in order to prevent the kaolinite units from curving. All these structural investigations of amesite were carried out using the powder method. Brindley, Oughton & Youell (1951) found a few small fragments in the material originally investigated by Gruner which were suitable for single-crystal techniques. Even the best single crystals which they used in their structure determination showed considerable disorder in the direction of the  $b$  axis. The present crystal-structure

analysis was carried out on a material from a different locality and on single crystals free from disorder.

### Experimental

The specimen of amesite was obtained from the National Museum in Washington, D.C., and bears the identifying number 103312. This specimen came from the Saranovskoye chromite deposit, North Urals, U.S.S.R. The crystal fragments are hexagonal prisms elongated parallel to the  $c$  axis. The crystals are pale green to colorless, and are transparent except in cases where a reddish deposit coats the surface.

With few exceptions, all amesite crystals studied were biaxial twins with

$$n_x = 1.597, n_y = 1.600, n_z = 1.615.$$

The optic plane is parallel to some complex  $(hki0)$  plane inclined 20° to the  $a$  axis. The optic angle  $2V$  is 10–14° and the optic sign is positive. The extinction angle in the basal section ( $X:a$ ) is 20°, and  $Z = c$  (Fig. 1(a)). The twins are trillings of equilateral triangles similar to aragonite. The twins range from simple arrangements of six segments joined on  $\{10\bar{1}0\}$  (Fig. 1(b)) to very complex arrangements joined on sutured faces.

The biaxial appearance of the crystals in polarized light must be due to strain because the X-ray diffraction data show that amesite is hexagonal. The observed extinctions in thick crystals looking down the  $c$  axis are sharp, but a thin cleavage fragment under similar conditions is faintly undulous.

X-ray diffraction data from a single untwinned crystal of amesite with dimensions of approximately  $0.1 \times 0.1 \times 0.2$  mm. were collected with both the Weissenberg and the precession cameras, using  $Cu K\alpha$  and  $Mo K\alpha$  radiation respectively. The diagrams were

\* Publication No. 63, Shell Development Company, Exploration and Production Research Division, Houston, Texas, U.S.A.

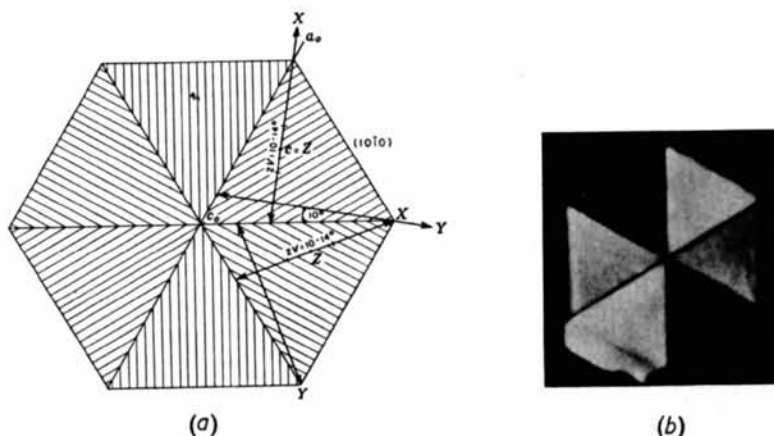


Fig. 1. (a) A sketch of the plane (0001) showing the twin segments, the optic plane and the vibration directions. (b) Photomicrograph of amesite, identical to sketch in (a); crossed nicols.

indexed on the basis of a hexagonal unit cell with dimensions

$$a = 5.31 \pm 0.01, \quad c = 14.04 \pm 0.02 \text{ \AA}.$$

Reflections of the type (000*l*) with *l* odd are systematically absent from the single-crystal diffraction diagrams. The Laue symmetry is 6/*m*; the diffraction symbol is therefore 6/*m*P6<sub>3</sub>/*m*. The hexagonal unit cell contains two 'molecules' of the formula (Mg<sub>2</sub>Al)(SiAl)O<sub>5</sub>(OH)<sub>4</sub>; the calculated X-ray density is 2.70 g.cm.<sup>-3</sup> as compared with a reported density of 2.78 g.cm.<sup>-3</sup> for amesite from a different locality (Gruner, 1944). The atomic arrangement of amesite is related to the kaolinite structure (Brindley *et al.*, 1951) which does not have a center of symmetry, and the acentric space group P6<sub>3</sub> is probably correct.

The distribution of intensities in the (0*kil*) zone lies well above the normal distribution curves (Fig. 2(a))

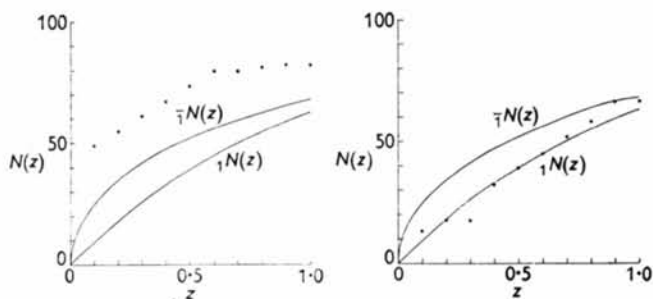


Fig. 2. (a) The observed distribution (dots) of intensities in the (0*kil*) zone, and the theoretical distributions (solid lines) for an acentric set,  ${}_1N_1(z)$ , and for a centric set,  ${}_1N_2(z)$ , of intensities. (b) The observed intensity distribution (dots) for the set of reflections  $(2h, \bar{h}, \bar{h}, l)$ .

because of the hypersymmetry (Rogers & Wilson, 1953) which mica-type structures display in the (0*kil*) projection, i.e. the atoms are arranged along lines at intervals of  $\frac{1}{3}b$ . The distribution of intensities in the  $(2h, \bar{h}, \bar{h}, l)$  zone—(*h*0*l*) for the orthohexagonal cell—

follows the acentric distribution (Howells, Phillips & Rogers, 1950) (Fig. 2(b)) and gives additional support to the choice of the non-centrosymmetric space group. The subsequent refinement of the structure shows that this space group is correct.

The relative intensities of reflections were determined by visual comparison with calibrated intensity strips. Multiple-film techniques were used in the case of the Weissenberg diagrams, and precession diagrams were exposed for a series of fixed time intervals to make certain that all intensities were on a linear scale. The usual Lorentz and polarization corrections were applied to the measured intensities.

#### Determination of the structure

Because the agreement between the observed and calculated structure factors as given in Brindley's article was good, it was decided to compute phases for a (0*kil*) projection using Brindley's positions of the atoms which he had placed according to the space group P6<sub>3</sub>*cm*. An electron-density projection was computed and although peaks were recovered at positions at which atoms had been assumed, their heights were unequal and there was a high electron-density peak at  $y = 0, z = 0.300$ , and a lower peak at  $y = \frac{1}{3}, z = 0.267$ . The first peak had a *z* coordinate identical with those chosen for the silicon atoms, and the second peak had a *z* coordinate which agreed with those for oxygens forming the base of the tetrahedron. However, the *y* coordinates could not be accounted for. Also, all the observed (0*kil*) reflections with  $l = 2n + 1$  were identically equal to zero for this structure. It is evident that in spite of the rather good agreement between the observed and calculated (0*kil*),  $l = 2n$ , structure factors for this atomic arrangement, the (0*kil*) Fourier analysis indicated that the postulated stacking of the kaolinite layers was incorrect. In Brindley's proposed structure, the sixfold axis passes through an OH group located at the level of the apical

oxygens of the  $\text{SiO}_4$  tetrahedra, and the silicons are located on the two threefold axes in the unit cell. The next layer in the unit cell is placed on top of the lower layer so that the equivalent hydroxyl groups have the same  $(x, y)$  parameters but are  $\frac{1}{2}z$  apart. If the upper layer is pivoted  $60^\circ$  about this hydroxyl, then a structural arrangement is obtained which fits into space group  $P6_3cm$ . The  $(0kil)$  projection shows this to be incorrect. The interpretation of this projection requires one silicon on the sixfold axis and the hydroxyl in place of the silicon on the threefold axis in the unit cell. If the upper layer is now rotated  $60^\circ$  with respect to the lower one, a structure is obtained which displays a  $P6_3$  symmetry, in agreement with the observed space group. However, it was noted that the  $(hki0)$  projection of this postulated structure had mirror planes along the diagonals of the unit cell. The absence of this diagonal mirror in the  $(hki0)$  diffraction pattern means that in the final structure some of the atoms will have coordinates which must differ from the postulated ideal positions.

The non-centrosymmetric  $(0kil)$  projection was evaluated using the 'ideal'  $x$  and  $y$  coordinates of the atoms in the positions as shown in Table 1.

Table 1. First trial positions of atoms in amesite

Atom	$x$	$y$	$z$	No. of equivalent atoms
Mg	$\frac{2}{3}$	0	0	6
Si <sub>1</sub>	0	0	0.306	2
Si <sub>2</sub>	$\frac{2}{3}$	$\frac{1}{3}$	0.306	2
O <sub>1</sub>	0	0	0.425	2
O <sub>2</sub>	$\frac{2}{3}$	$\frac{1}{3}$	0.425	2
O <sub>3</sub>	$\frac{1}{3}$	$\frac{1}{3}$	0.267	6
OH <sub>1</sub>	$\frac{1}{3}$	$\frac{2}{3}$	0.425	2
OH <sub>2</sub>	$\frac{1}{3}$	0	0.075	6

The agreement was good between all observed and calculated  $(0kil)$  structure factors for this first trial structure ( $R = 0.186$ ). The first  $(0kil)$  projection, showed that all the atoms were in essentially correct positions. The final projection is shown in Fig. 3. The electron density was sampled in intervals of  $\frac{1}{60}$  along  $a_2$  and in intervals of  $\frac{1}{120}$  along  $c$ .

Before further refinement of this projection was undertaken, it was decided to evaluate an  $(hki0)$  Fourier series in an attempt to learn which atoms must be moved from the 'ideal'  $x$  and  $y$  coordinates to account for the absence of a mirror plane along the diagonal in this projection.

Using the 'ideal'  $x$  and  $y$  parameters, signs for the  $F(hki0)$  structure factors were evaluated. For the postulated model of amesite, the calculated structure factor of the reflection  $(hki0)$  was identical with that for the reflection  $(khi0)$ . The  $(hki0)$  projection (Fig. 4) showed that the  $y$  coordinate of the oxygen atom forming the base of the  $\text{SiO}_4$  tetrahedron moved considerably from its ideal value of 0.167; all other atoms were recovered at the positions at which they had been

placed. In order to improve the resolution of this projection, the magnesium contributions to the  $(hki0)$  structure factors were subtracted and a new  $(hki0)$  projection was computed with these modified coefficients. The previously noted shift of the  $y$  parameter towards a higher value was confirmed by this projection. Because of the large amount of overlap present in this projection, it was decided to refine this zone by systematically varying the  $y$  parameter of this oxygen atom and to plot the changes of the coordinate against

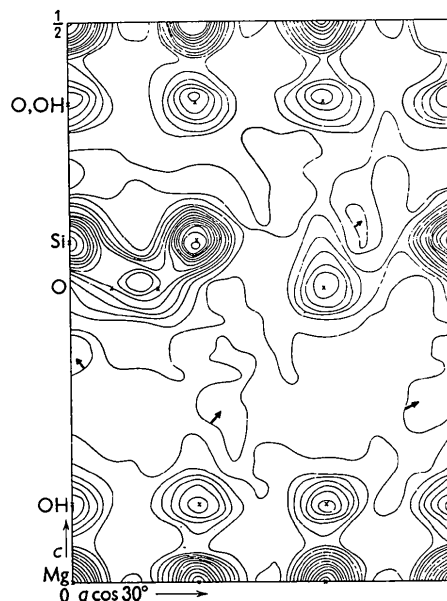


Fig. 3. The  $(0kil)$  electron-density projection of amesite. Contours at intervals of approximately  $2 \text{ e.}\text{\AA}^{-2}$ . Crosses mark the final positions of the atoms. Negative regions are indicated by arrows.

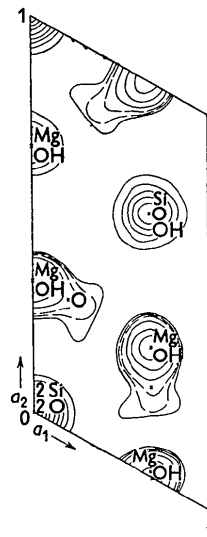


Fig. 4. The  $(hki0)$  electron-density projection of amesite. Contours at approximately  $10 \text{ e.}\text{\AA}^{-2}$  starting at  $10 \text{ e.}\text{\AA}^{-2}$ . The 12 and  $14 \text{ e.}\text{\AA}^{-2}$  contours are shown dashed in the region of overlap.

the discrepancy coefficient,  $R$ . A minimum,  $R=0.186$ , was observed for  $y = 0.230$  and this was taken as the correct position for the oxygen. It was not possible to determine from projections alone whether the coordinates of the other atoms deviate from their ideal values, because of the overlap of atoms present in this view of the structure. However, the oxygen deviation was apparent since it is the only atom which appears fairly well resolved in this projection. The displacement of this oxygen from the 'ideal' value  $y = 0.167$  destroys the diagonal mirror which was present in the  $(hki0)$  projection of the ideal structure, and the calculated and observed intensities agree quite well. The final value of the discrepancy coefficient for this projection is 0.176.

The  $(Okil)$  structure factors were recomputed, using the value  $y$  for oxygen obtained from the  $(hki0)$  projection. The  $R(Okil)$  dropped from 0.186 to 0.137. Back-shift corrections for the lack of convergence of the Fourier series were applied to the  $z$  parameters and the structure factors were recomputed once more. The final value of the discrepancy factor was  $R(Okil) = 0.113$ . The final coordinates of the atoms are listed in Table 2.

Table 2. *Final atomic coordinates of amesite*

Atom	$x$	$y$	$z$
Mg	0.667	0	0
Si <sub>1</sub>	0	0	0.306
Si <sub>2</sub>	0.667	0.333	0.306
O <sub>1</sub>	0	0	0.428
O <sub>2</sub>	0.667	0.333	0.428
O <sub>3</sub>	0.333	0.230	0.265
OH <sub>1</sub>	0.333	0.667	0.428
OH <sub>2</sub>	0.333	0	0.072

Calculated and observed values of  $|F|$  are listed in Table 3. The atomic scattering factors given by James & Brindley were used; for atoms in tetrahedral positions, the weighted scattering factor was  $\frac{1}{2}[f_{Si} + f_{Al}]$  and for atoms in octahedral positions it was  $\frac{1}{3}[2f_{Mg} + f_{Al}]$ . The calculated structure factors were adjusted by multiplication by a temperature factor  $\exp[-\beta \sin^2 \theta / \lambda^2]$ .  $\beta$  was evaluated graphically from the slope of a plot of  $\ln F_o / F_c$  versus  $\sin^2 \theta / \lambda^2$  and was  $1.7 \text{ \AA}^2$ .

#### Effect of heat treatment of amesite

A single crystal of amesite was heated at  $650 \pm 25^\circ \text{C}$ . for ten days and then quenched to room temperature. The diffraction diagram of the  $(Okil)$  zone (Fig. 5) showed a strong diffuse reflection at a position where the  $(0001)$  reflection would be if it had been present. Another very strong diffuse reflection was observed in the region of the  $(0005)$  reflection. This would be at a  $d_{hki0}$  value of about  $2.8 \text{ \AA}$  and explains the observation of Brindley *et al.* (1951) of this line in the powder diagram which they thought might be due to the mineral fayalite. Diffuse reflections of lesser

Table 3. *Calculated and observed structure factors*

<i>Okil zone; acentric</i>					
<i>Okil</i>	$ F_c $	$F_o$	<i>Okil</i>	$ F_c $	$F_o$
0000	280	—	03 $\bar{3}$ 0	98	84
2	56	59	2	38	33
4	96	94	4	38	39
6	47	46	6	24	25
8	27	33	8	17	13
10	39	41	10	33	30
12	37	33	12	23	25
14	32	33	14	26	25
16	33	36	16	24	28
01 $\bar{1}$ 0	17	17	04 $\bar{4}$ 0	4	7
1	28	25	1	5	7
2	16	13	5	7	7
3	23	18	7	8	7
4	12	13	9	7	7
5	18	16	11	7	7
6	9	10	15	4	7
7	12	13	—	—	—
8	6	7	05 $\bar{5}$ 9	6	7
9	9	10	11	6	7
10	4	5	—	—	—
11	6	7	06 $\bar{6}$ 0	28	28
12	3	5	2	12	10
13	5	7	4	11	13
—	—	—	6	9	13
02 $\bar{2}$ 0	3	7	—	—	—
1	6	10	—	—	—
2	5	5	—	—	—
3	12	13	—	—	—
4	9	7	—	—	—
5	17	13	—	—	—
6	10	10	—	—	—
7	18	16	—	—	—
8	11	10	—	—	—
9	18	18	—	—	—
10	10	10	—	—	—
11	15	16	—	—	—
12	8	7	—	—	—
13	12	10	—	—	—
14	6	5	—	—	—
15	9	7	—	—	—
16	4	5	—	—	—
17	6	7	—	—	—
<i>hki0 zone; centric</i>					
<i>hki0</i>	$F_c$	$F_o$	<i>hki0</i>	$F_c$	$F_o$
1000	17	17	12 $\bar{3}$ 0	17	16
2	—3	7	2	28	19
3	98	84	3	1	2
4	4	7	4	5	8
6	28	28	—	—	—
—	—	—	13 $\bar{4}$ 0	18	15
11 $\bar{2}$ 0	15	15	2	5	4
2	2	2	3	40	46
3	—1	4	—	—	—
4	9	8	14 $\bar{5}$ 0	9	7
5	7	8	—	—	—

intensities can also be seen close to the 6th and 10th orders of  $(000l)$  of amesite, as well as in other regions of the  $(Okil)$  zone.

The diffuse streaks which can be seen along the lines for which  $k \neq 3n$  indicate that the heat treatment has introduced a randomness in the stacking of

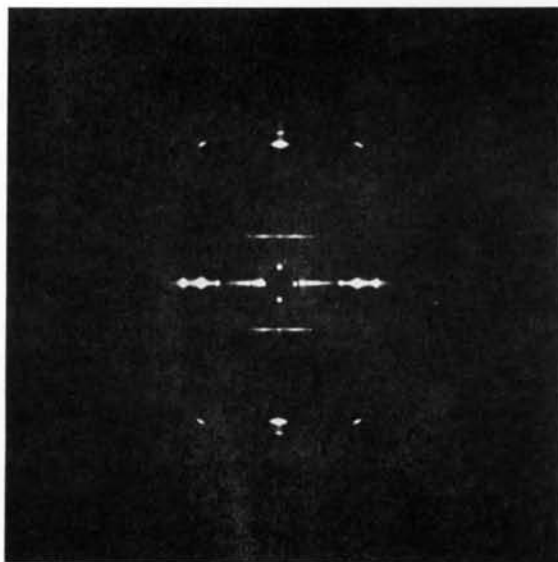


Fig. 5. Precession diagram of the  $(0kil)$  zone of amesite after 10 days heating at  $650^{\circ}\text{C}$ .

the layers typical of that usually found in micaceous minerals.

### Discussion

Amesite is a hydrated silicate of magnesium and aluminum with possibly some iron replacing magnesium in the octahedral position. Its ideal formula can be written as  $(\text{Mg}_2\text{Al})(\text{SiAl})\text{O}_5(\text{OH})_4$ . For many years this mineral was classified as belonging to the chlorite group, and Winchell (1951) lists it as one of the four end members in terms of which the composition of all chlorites can be explained. Gruner (1944), however, showed that the X-ray diffraction intensities of the  $(000l)$  basal reflections can be accounted for only by a sequence of atomic planes similar to the sequence of planes found in the structure of kaolinite. An examination by Brindley *et al.* (1951) of the amesite specimen on which Gruner had done powder work enabled these workers to pick out small crystal fragments which provided information for an attempt at a more exact determination of this structure. The diffraction photographs which they obtained showed spectra which were sharp only when the Miller index  $k$  was an integral multiple of three, while all other spots appeared as streaks. The appearance of such streaks on diffraction photographs of minerals having a layer structure indicates that the sheets are randomly stacked with displacements which are a sub-multiple of a particular lattice translation. The special groups of spectra which do not reflect this disorder will usually display a higher diffraction symmetry than is actually possessed by the crystal, and a structure determination based on such data will be only an approximation to the true atomic arrangement. Thus reflections of the type  $(hki)$ ,  $k \neq 3n$ , assume great

prominence in this investigation. The diffraction diagrams of the amesite specimen used in this determination showed that all types of spectra consisted of sharp spots and it was evident that a stacking of layers as postulated by Brindley was incorrect.

The sequence of atomic planes in the  $c$  direction for one layer of the amesite structure is the same as for a kaolinite unit (Pauling, 1930) except that all octahedral positions are occupied; aluminum and silicon atoms fill the tetrahedral sites and one aluminum and two magnesium atoms fill the octahedral sites.

Table 4 lists the bond lengths and angles obtained from the coordinates of Table 3.

Table 4. Bond lengths and angles in amesite

	Length (Å)		Angle ( $^{\circ}$ )
$\text{Si}_1\text{-O}_1$	$1.71 \pm 0.03$	$\text{O}_1\text{-Si-O}_3$	$110 \pm 2$
$\text{Si}_1\text{-O}_3$	$1.67 \pm 0.02$	$\text{O}_3\text{-Si-O}_3$	$109 \pm 2$
$\text{Mg-OH}$	$2.04 \pm 0.02$	$\text{Si-O}_3\text{-Si}$	$133 \pm 2$
$\text{O} \cdots \text{O}^*$	$2.72 \pm 0.02$	—	—
$\text{O}_3 \cdots \text{H} \cdots \text{O}$	$2.97 \pm 0.03$	—	—

\* Tetrahedral.

The probable errors are estimates based on the back-shift corrections, which did not exceed  $0.03 \text{ \AA}$ , and also on the fact that some of the  $(hki)$  intensities are extremely sensitive to very small changes in the basal oxygen parameter,  $y$ .

It is to be noted that the hexagon formed by the oxygens in the base of the  $\text{SiO}_4$  tetrahedra has expanded so that its side is  $2.72 \text{ \AA}$  instead of  $2.66 \text{ \AA}$  for the ideal structure. The  $\text{Si-O}_3$  bond has a value of  $1.67 \text{ \AA}$  as compared to the value  $1.60 \text{ \AA}$  for  $\text{Si-O}$  in quartz. The lengthening of this bond and the expansion of the oxygen hexagon is due to the replacement of silicon ( $r = 0.41 \text{ \AA}$ ) by aluminum ( $r = 0.50 \text{ \AA}$ ) in the tetrahedral positions. Smith (1954) has summarized all the published  $\text{Si-O}$  and  $\text{Al-O}$  bond lengths reported for structures which contained various ratios of Al and Si in tetrahedral position. He found that a plot of the  $\text{Si}_x\text{Al}_y\text{-O}$  bond length against the percent Si was linear. The bond lengths for this bond when one-half of the silicon is replaced by aluminum, as found from this graph, is  $1.69 \text{ \AA}$ . The observed bond length in amesite,  $1.67 \text{ \AA}$ , is close enough to show that almost one-half of the silicon is replaced by aluminum.

The hexagon formed by the apical oxygens of the  $\text{SiO}_4$  tetrahedra is rotated  $30^{\circ}$  from that of the bottom hexagon and its edge is  $3.06 \text{ \AA}$  (Fig. 6). Using the value  $2.72 \text{ \AA}$  for the lower hexagon and computing the length of an edge of a hexagon rotated  $30^{\circ}$  and having its sides bisected by the corners of the lower hexagon yields a value of  $3.04 \text{ \AA}$ . Thus the packing of the two oxygen layers is accomplished with hardly any strain. The slight rotation of the triad of oxygens in the base of the tetrahedron (Fig. 6) lengthens the bond between this atom and the oxygen above it from  $2.75 \text{ \AA}$ , based on the ideal coordinates, to  $2.77 \text{ \AA}$ . Apparently

the slight increase in this distance eliminates any strains still remaining after the adjustments due to the isomorphous replacement.

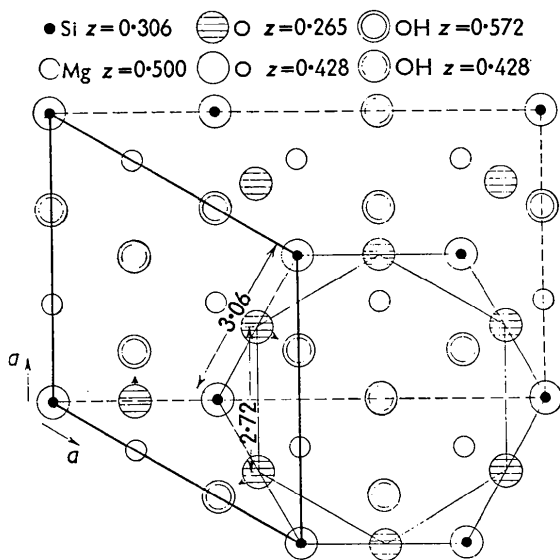


Fig. 6. Projection of one layer of amesite on the (0001) plane. Arrows indicate the direction of motion of the oxygens away from the ideal positions. The dashed lines outline the orthohexagonal cell.

The bond length between silicon and the apical oxygen is 1.71 Å and is longer than the Si–O length in the base because this oxygen is shared between a tetrahedron and an octahedron.

The O–Si–O angles are tetrahedral and the Si–O–Si angle is 133°. The closest approach between the oxygen forming the base of the SiO<sub>4</sub> tetrahedron and the hydroxyl in the layer below it is 2.97 Å. In kaolinite, two-thirds of the O···H···O distances are found to be 2.99 Å and the remaining third 2.87 Å (Brindley & Robinson, 1946). In all these structures, the hydrogen bonds play an important role in holding the layers together.

The two layers in the unit cell of amesite are related by a 60° rotation about the sixfold axis passing through the two equivalent silicon atoms.

The ideal position of O<sub>3</sub>, namely  $x = \frac{1}{3}$ ,  $y = \frac{1}{6}$ , implies that reflections ( $hki0$ ) and ( $khi0$ ) should have equal intensities. In addition, only the silicon atoms on the threefold axis and the oxygens in the base of the tetrahedron contribute to the ( $0kil$ ) structure factors with  $l = 2n+1$ . Thus, relatively small changes in the oxygen positions will influence these structure factors considerably. This is reflected in the value of the discrepancy coefficient for the 24 observed

( $0kil$ ),  $l = 2n+1$ , reflections, which dropped from 0.255 ( $x = \frac{1}{3}$ ,  $y = \frac{1}{6}$ ) to 0.152 for  $x = \frac{1}{3}$ ,  $y = 0.230$ . An even more sensitive test is provided by sets of reflections such as (2130), (12 $\bar{3}$ 0) and (3140), (13 $\bar{4}$ 0). In every case, the magnesium contributions are very small and all the oxygen and hydroxyl contributions, except from those in the base of the tetrahedron, almost cancel. The silicon atoms, because of their positions, make equal contributions to these reflections; thus the intensities become very sensitive to the parameters of the basal oxygens.

Satisfactory agreement is reached only when the oxygen is moved away from the position  $y = \frac{1}{6}$ , and a systematic variation of the  $y$  parameter shows best agreement for  $F_o$  and  $F_c$  for  $y = 0.230$ . It is quite possible that similar deviations of atoms from their ideal positions in the crystal structure of dickite (Hendricks, 1938) will correctly account for the hitherto unexplained intensities of the (020), (021), and (022) reflections.

The intensities ( $03\bar{3}l$ ),  $l = 2n+1$ , are equal to zero for the ideal structure of amesite. However, when the oxygen is displaced from  $y = \frac{1}{6}$ , it will begin to make an intensity contribution to reflections of this type. The calculated contribution to the structure factors for ( $03\bar{3}1$ ), ( $03\bar{3}3$ ), and ( $03\bar{3}5$ ) is so small that it should not be possible to observe reflections of this type. A very heavily over-exposed ( $0kil$ ) diffraction diagram was examined for the appearance of any of these reflections. There was a very faint indication of a ( $03\bar{3}1$ ) reflection, but even such a faint reflection could not be explained entirely by the oxygen contribution. Only three-dimensional sections through the planes of the atoms could show what other atomic deviations from the ideal might exist in the structure of amesite.

## References

- BRINDLEY, G. W., OUGHTON, B. M. & YUELL, R. F. (1951). *Acta Cryst.* **4**, 552.  
 BRINDLEY, G. W. & ROBINSON, U. (1946). *Miner. Mag.* **27**, 242.  
 GRUNER, J. W. (1944). *Amer. Min.* **29**, 422.  
 HENDRICKS, S. B. (1938). *Amer. Min.* **23**, 295.  
 HOWELLS, E. R., PHILLIPS, D. C. & ROGERS, D. (1950). *Acta Cryst.* **3**, 210.  
 McMURCHY, R. C. (1934). *Z. Kristallogr.* **88**, 420.  
 PAULING, L. (1930). *Proc. Nat. Acad. Sci., Wash.* **16**, 578.  
 ROGERS, D. & WILSON, A. J. C. (1953). *Acta Cryst.* **6**, 439.  
 SMITH, J. V. (1954). *Acta Cryst.* **7**, 479.  
 WINCHELL, A. N. (1951). *Elements of Optical Mineralogy*. New York: Wiley.